



OPEN

Effects of empagliflozin and target-organ damage in a novel rodent model of heart failure induced by combined hypertension and diabetes

Kristin Kräker^{1,2,3,4,5,13}, Florian Herse^{1,2,3,5,13}, Michaela Golic^{1,2,3,4,5}, Nadine Reichhart⁶, Sergio Crespo-Garcia^{6,7}, Olaf Strauß⁶, Jana Grune^{4,8,9,10}, Ulrich Kintscher^{4,9}, Manal Ebrahim¹¹, Michael Bader^{2,3,4,5}, Natalia Alenina^{3,4}, Arnd Heuser³, Friedrich C. Luft^{1,3,4}, Dominik N. Müller^{1,2,3,4,5}, Ralf Dechend^{1,2,5,12,13}✉ & Nadine Haase^{1,2,3,4,5,13}

Type 2 diabetes mellitus and hypertension are two major risk factors leading to heart failure and cardiovascular damage. Lowering blood sugar by the sodium-glucose co-transporter 2 inhibitor empagliflozin provides cardiac protection. We established a new rat model that develops both inducible diabetes and genetic hypertension and investigated the effect of empagliflozin treatment to test the hypothesis if empagliflozin will be protective in a heart failure model which is not based on a primary vascular event. The transgenic Tet29 rat model for inducible diabetes was crossed with the mRen27 hypertensive rat to create a novel model for heart failure with two stressors. The diabetic, hypertensive heart failure rat (mRen27/tetO-shIR) were treated with empagliflozin (10 mg/kg/d) or vehicle for 4 weeks. Cardiovascular alterations were monitored by advanced speckle tracking echocardiography, gene expression analysis and immunohistological staining. The novel model with increased blood pressure and higher blood sugar levels had a reduced survival compared to controls. The rats develop heart failure with reduced ejection fraction. Empagliflozin lowered blood sugar levels compared to vehicle treated animals (182.3 ± 10.4 mg/dl vs. 359.4 ± 35.8 mg/dl) but not blood pressure (135.7 ± 10.3 mmHg vs. 128.2 ± 3.8 mmHg). The cardiac function was improved in all three global strains (global longitudinal strain $-8.5 \pm 0.5\%$ vs. $-5.5 \pm 0.6\%$, global radial strain $20.4 \pm 2.7\%$ vs. $8.8 \pm 1.1\%$, global circumferential strain $-11.0 \pm 0.7\%$ vs. $-7.6 \pm 0.8\%$) and by increased ejection fraction ($42.8 \pm 4.0\%$ vs. $28.2 \pm 3.0\%$). In addition, infiltration of macrophages was decreased by treatment (22.4 ± 1.7 vs. 32.3 ± 2.3 per field of view), despite mortality was not improved. Empagliflozin showed beneficial effects on cardiovascular dysfunction. In this novel rat model of combined hypertension and diabetes, the improvement in systolic and diastolic function was not secondary to a reduction in left ventricular mass or through modulation of the afterload, since blood pressure was not changed. The mRen27/tetO-shIR strain should provide utility in separating blood sugar from blood pressure-related treatment effects.

¹Experimental and Clinical Research Center, Lindenberger Weg 80, 13125 Berlin, Germany. ²Berlin Institute of Health (BIH), Berlin, Germany. ³Max-Delbrück Center for Molecular Medicine in the Helmholtz Association, Berlin, Germany. ⁴DZHK (German Centre for Cardiovascular Research), Berlin, Germany. ⁵Charité – Universitätsmedizin Berlin, Berlin, Germany. ⁶Experimental Ophthalmology, Department of Ophthalmology, Charité – Universitätsmedizin Berlin, Berlin, Germany. ⁷Department of Biochemistry, Université de Montréal, Montreal, Canada. ⁸Institute of Physiology, Charité – Universitätsmedizin Berlin, Berlin, Germany. ⁹Institute of Pharmacology, Center for Cardiovascular Research, Charité – Universitätsmedizin Berlin, Berlin, Germany. ¹⁰Center for Systems Biology, Massachusetts General Hospital, Harvard Medical School, Boston, USA. ¹¹Technische Universität Berlin, Berlin, Germany. ¹²HELIOS-Klinikum, Berlin, Germany. ¹³These authors contributed equally: Kristin Kräker, Florian Herse, Ralf Dechend and Nadine Haase. ✉email: ralf.dechend@charite.de

Abbreviations

Anp	Atrial natriuretic peptide (gene)
Bnp	Brain natriuretic peptide (gene)
BNP	Brain natriuretic peptide (protein)
Col1	Collagen type 1
Ctgf	Connective tissue growth factor (gene)
DOX	Doxycycline
ED1	CD68 ⁺ macrophages
EF	Ejection fraction
empa	Empagliflozin
FN	Fibronectin
FS	Fractional shortening
GCS	Global circumferential strain
GLS	Global longitudinal strain
GRS	Global radial strain
HF	Heart failure
HFpEF	Heart failure with preserved ejection fraction
HFrfEF	Heart failure with reduced ejection fraction
IVSd	Interventricular septum, diastole
LV	Left ventricular
LVPWd	Left ventricular posterior wall, diastole
MAP	Mean arterial blood pressure
mRen27	Hypertensive rat model
mRen27/tetO-shIR	Hypertensive, diabetic heart failure rat model
mRNA	Messenger ribonucleic acid
Myh6/7	Myosin heavy chain 6/7
RT-PCR	Real-time polymerase chain reaction
SD	Sprague Dawley
SEM	Standard error of the mean
SGLT2	Sodium-glucose co-transporter 2
SHR	Spontaneously hypertensive rats
Tet29	Diabetic rat model (tetO-shIR)

Systolic blood pressure, smoking and glucose concentrations are the three main risk factors for cardiovascular disease in that order¹. Type 2 diabetes mellitus combined with hypertension is associated with an enhanced risk, demonstrating the catastrophic combination of these two risk factors². Indeed, hypertension is present in over two-thirds of type 2 diabetes mellitus patients. Hypertension and type 2 diabetes mellitus together meld in heart failure. The prognosis is especially poor in type 2 diabetes mellitus patients because of cardiovascular end organ damage, leading to myocardial fibrosis and diastolic dysfunction³. Patients suffering from type 2 diabetes mellitus exhibit subclinical cardiac dysfunction and renal impairment. However, some glucose-lowering therapies actually increase hospital admissions^{4,5}. It is known that lowering blood pressure has a dramatic effect on cardiovascular endpoints at all ages. In type 2 diabetes mellitus, the results are less clear⁶. A new class of oral anti-diabetic drugs, sodium-glucose co-transporter 2 (SGLT2) inhibitors, lowers blood glucose in an insulin-independent manner, by inhibiting renal glucose reabsorption in the proximal tubule. The recent Empagliflozin Cardiovascular Outcome Event Trial in type 2 diabetes (EMPA-REG OUTCOME) documented the impressive benefits obtained with empagliflozin (empa)⁷. Empa reduced the primary composite outcome of cardiovascular death, non-fatal myocardial infarction or non-fatal stroke (3-point major adverse cardiovascular events), hospitalization for heart failure, and overall mortality compared with placebo⁷. Myocardial infarction and stroke remained unchanged with therapy, suggesting effects not related to thrombosis⁸. The fact that SGLT2 inhibitors reduce cardiovascular events by reducing primarily heart failure has appeal⁹. New ESC guidelines on chronic coronary syndrome favor SGLT2 inhibitors as primary medication in untreated patients with diabetes before inducing metformin¹⁰. However, metformin was the primary medication before applying empa in the clinical studies. The question now is whether empa is also cardio protective if administered as the only antidiabetic agent? Several other questions remained unanswered, such as the mechanism of action. An animal model of both hypertension and diabetes might have more utility than either condition alone. We generated a novel rodent model for heart failure by mating rats with type 2 diabetes and hypertension^{11,12}. Heart-failure is induced by two stressors, hypertension and diabetes, with state-of-the art technology^{13,14}.

The transgenic Tet29 rat model in which the insulin receptor is ubiquitously knocked down via doxycycline (dox)-induced RNA interference (small hairpin RNA), leading to insulin resistance and type 2 diabetes mellitus¹¹ is crossed to the mRen27 rat. Transgenic rats carrying the murine Ren27 gene represent a monogenetic model of hypertension induced end organ damage characterized by low plasma renin and high extra renal expression of the transgene¹². It remains an unanswered question from the clinical trials whether the positive effects of SGLT2 inhibitors on heart failure occur predominantly in heart failure with a preserved ejection fraction (HFpEF) or heart failure with a reduced ejection fraction (HFrfEF).

Methods

Animal studies. All animal experiments were performed according to national and international guidelines and were approved by local authorities (State Office of Health and Social Affairs Berlin). We used 18 weeks old and body weight-matched male rats to characterize a new rat model for hypertensive and diabetic heart failure.

For this purpose, Sprague Dawley healthy control rats (SD; $n = 5$), diabetic rats (tetO-shIR; $n = 10$)¹¹, hypertensive rats (mRen27; $n = 9$)¹², and crossbred diabetic and hypertensive rats (mRen27/tetO-shIR; $n = 5$) were monitored for 9 weeks. All animals were bred at the Max-Delbrück Center for Molecular Medicine Berlin, Germany. Type 2 diabetes mellitus in the tetO-shIR and mRen27/tetO-shIR rats was induced by oral doxycycline (dox) application. TetO-shIR and mRen27/tetO-shIR rats received 2 mg/kg/d dox via drinking water until they were hyperglycemic with blood glucose level of between 300 and 400 mg/dL. Afterwards, 0.5 mg/kg/d dox was given to maintain the blood glucose level at that level over the entire period of 9 weeks. SD and mRen27 received water. After 8 weeks, blood pressure was monitored by tail cuff measurements and echocardiography was done. Blood glucose was measured manually with the Accu-Chek Aviva blood glucose meter (Roche, Germany) once a week. For the investigation of the effects of empa, 18 weeks old, age-matched and body weight-matched male mRen27/tetO-shIR rats were used. Type 2 diabetes mellitus was induced by dox as described above for 5 weeks. Afterwards, rats were randomly assigned to 2 experimental groups, vehicle-treated (water; $n = 13$) or treated with 10 mg/kg/d empa in the drinking water ($n = 14$). The treatment period was 4 weeks. At the end of the study rats were sacrificed by decapitation with prior anesthesia using isoflurane or due to predefined stopping criteria according with the European law for animal protection. Serum brain natriuretic peptide (BNP) was quantified according to the assay manual provided by the manufacturer (Abcam). The experimental unit is described by one single animal.

Echocardiography. As previously described¹⁵, transthoracic echocardiography was performed under anesthesia (induction in a chamber with 2%, continuation with 1–1.5% isoflurane) on a tiltable, heated platform to maintain 37 °C body temperature, executed by a single examiner blinded to the treatment groups ($n = 6–10$ rats per group). Chest hair was gently removed using a clipping machine and depilatory cream. A VisualSonics VEVO 2,100 imaging system with a 21 MHz transducer (MS250) mounted on an integrated rail system was used, simultaneously recording an electrocardiogram. M-mode and B-mode images were obtained in parasternal short and long axes views for measurement of diastolic left ventricular (LV) wall thickness (IVSd, LVPWd) and LV systolic function (EF, FS), respectively. Images were acquired and stored for offline analysis. Offline myocardial strain imaging analysis was performed by an investigator unaware of treatments using VisualSonics Vevo Strain software version 2.2.0 (Toronto, Canada) with a speckle tracking algorithm. B-Mode cine loops were checked for image quality with regard to differentiation of wall borders and absence of artefacts. Strain analysis was performed on three consecutive cardiac cycles. The endocardium of the LV was traced manually in parasternal short- and long-axis view in end-diastole. The epicardium was automatically traced by the software, checked and manually adjusted if necessary for maximum tracking accuracy. Global strain values were obtained from the average of the six segments of the LV. Since echocardiography was performed under anesthesia due to animal welfare aspects and could therefore represent a limitation of this study, special attention was paid to a uniform procedure in the execution and evaluation of the data.

mRNA isolation and real-time RT-PCR. Total mRNA was isolated from the left ventricle of the heart ($n = 5$ per group) using QIAzol lysis reagent and Qiagen RNeasy mini kit (Qiagen) with on-column deoxyribonuclease I step (Qiagen) according to manufacturer's protocol as previously described¹⁶. 2 µg of mRNA was reverse transcribed into cDNA using High Capacity cDNA Reverse Transcription Kit (Applied Biosystems). Real-time polymerase chain reaction (RT-PCR) was detected on ABI 7500 Fast Sequence Detection System (Applied Biosystems) and analyzed by 7500 Fast System Software (Applied Biosystems). Primers and probes (Supplementary table 1) were designed with PrimerExpress 3.0 (Applied Biosystems) and synthesized by Biotex (Germany). Analysis of target mRNA expression was performed with RT-PCR using the relative standard curve method. The expression level of the target genes was normalized by the expression of the *18S* housekeeping gene. Samples were run in triplicates and mean was used for further calculations. The arbitrary units reflect the ratio of the target mRNA concentration divided by the concentration of *18S* of the same sample.

Blood pressure and blood glucose measurement. Blood pressure measurement was performed by non-invasive tail cuff (CODA High Throughput System, Kent Scientific Corp., Torrington, USA). Blood glucose was measured by taking capillary blood droplets from tail puncture (Accu-Chek Aviva blood glucose meter, Roche, Mannheim, DEU). The measurements are carried out by animal keepers with decades of experience in a quiet environment to keep the stress for the animals as low as possible.

Immunohistochemistry. Paraffin-embedded hearts (vehicle $n = 6$, empa $n = 8$) were cut 4–6 µm thick and stained. Immunohistological techniques were performed as previously described¹⁷. Heart sections were incubated with primary antibodies against rat macrophages (ED1; #MCA341R, Bio-Rad), fibronectin (FN; #ab23751, abcam), and collagen I (Col I; #131001, SouthernBiotech). Vectashield mounting medium with DAPI (#H-1200, Vector Laboratories) was used to stain nuclei. Semi-quantitative analyses of immunohistochemistry and histology were conducted without knowledge of the specific treatment and performed using Panoramic MIDI II slide scanner (3D Histech, Hungary), CaseViewer and Image J software. For the histological and cardiomyocyte analysis, 5 hearts of each group were examined. Picking out cardiac areas for immunohistochemistry were standardized and uniformly distributed over the entire cross-section. Ten to fifteen different areas of each heart were analyzed. For the determination of the perivascular fibrosis, all vessels in the left ventricle were evaluated.

Statistics. Normal distribution was assessed by Kolmogorov–Smirnov test. Group differences were analyzed by two-tailed unpaired *t*-test, Mann–Whitney *U* test, one-way ANOVA with Tukey post hoc test or two-way ANOVA with Bonferroni post hoc test, as appropriate. Survival was examined using a Kaplan–Meier analysis.

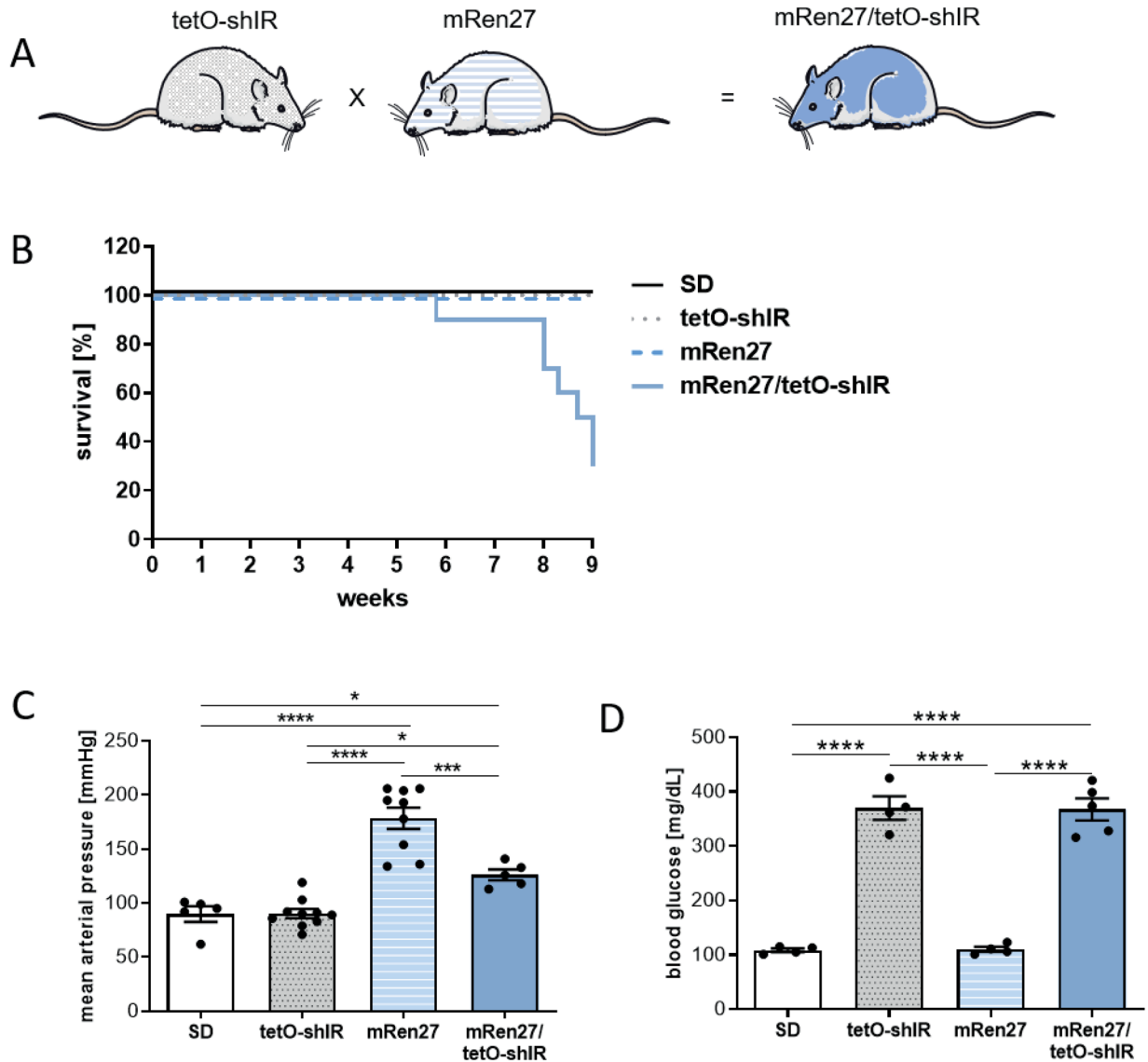


Figure 1. Characteristic of the new animal model. (A) Rat model for hypertensive and diabetic heart failure by breeding a hypertensive rat (mRen27), with an inducible diabetic rat (tetO-shIR) resulting in the hypertensive diabetic rat (mRen27/tetO-shIR). (B) Kaplan–Meier survival analysis of SD, diabetic (tetO-shIR), hypertensive (mRen27) and hypertensive diabetic rats (mRen27/tetO-shIR). At week 9, only 30% of hypertensive diabetic rats (mRen27/tetO-shIR) survived. Survival curves are statistically different by the log-rank test ($p < 0.0001$). No SD, diabetic (tetO-shIR) and hypertensive (mRen27) rats died before end of study. (C) Tail-cuff mean arterial pressure (MAP) was increased in mRen27 rats compared to SD, tetO-shIR and mRen27/tetO-shIR rats. The hypertensive diabetic rats (mRen27/tetO-shIR) showed significantly elevated MAP compared to SD and tetO-shIR rats. SD and tetO-shIR rats were normotensive. (D) Blood glucose level were significantly higher in tetO-shIR and mRen27/tetO-shIR rats compared to SD and mRen27 rats. 1-way ANOVA, * $p < 0.05$, *** $p < 0.001$, **** $p < 0.0001$; data expressed as mean \pm SEM.

The ROUT method was performed for outlier identification with an average false discovery rate less than 1%. A value of $p < 0.05$ was considered statistically significant. All data are presented as means \pm SEM. Numbers of evaluated animals are given in the method description.

Ethics approval. Local authorities approved the studies (State Office of Health and Social Affairs Berlin, Germany), predefined stopping criteria according with the European law for animal protection were included.

Results

Hypertension and diabetes share many features and often occur together. We therefore bred a hypertensive rat model, the mRen27 rat, with an inducible type 2 diabetes mellitus rat model to generate the mRen27/tetO-shIR rat (Fig. 1A). Hypertensive mRen27 rats and induced diabetic tetO-shIR rats exhibited no mortality in the investigated period. However, 9 weeks of combined hypertension and type 2 diabetes mellitus in mRen27/

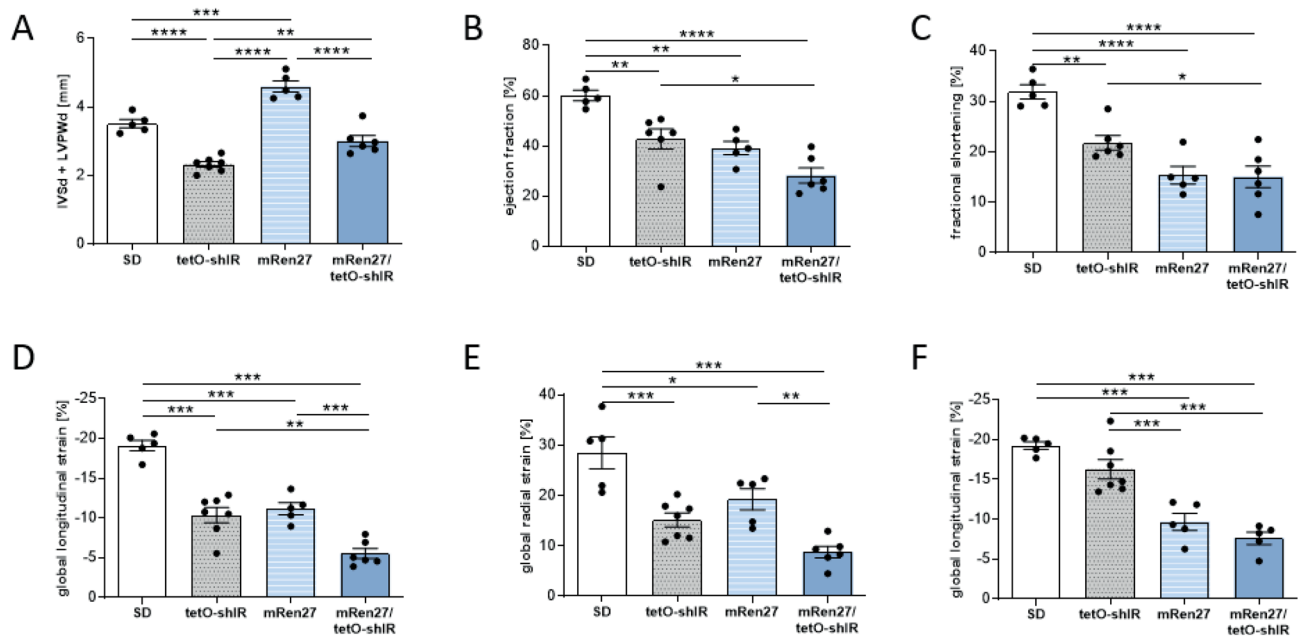


Figure 2. Functional analysis by Speckle Tracking Echocardiography. (A) Hypertensive rats (mRen27) showed an increased wall thickness (IVSd + LVPWd) compared to SD, tetO-shIR and mRen27/tetO-shIR rats. Diabetic (tetO-shIR) and hypertensive diabetic rats (mRen27/tetO-shIR) had no thickened cardiac walls. (B) Ejection fraction and (C) fractional shortening were significantly reduced in tetO-shIR, mRen27 and mRen27/tetO-shIR rats compared to SD. (D) Global longitudinal strain was significantly reduced in tetO-shIR, mRen27 and mRen27/tetO-shIR rats compared to SD, as were (E) global radial strain and (F) global circumferential strain. 1-way ANOVA, * $p < 0.05$, ** $p < 0.01$, *** $p < 0.001$, **** $p < 0.0001$; data expressed as mean \pm SEM.

tetO-shIR rats reduced survival by 30% (Fig. 1B). The mRen27 rats had high mean arterial blood pressure (178 ± 10 mmHg), whereas the diabetic rats (90 ± 4 mmHg) and SD rats (90 ± 7 mmHg) were normotensive. The hypertensive diabetic rats (126 ± 5 mmHg) had lower blood pressures compared to the hypertensive mRen27 rat; however, the values were still significantly higher compared to the normotensive SD rats (Fig. 1C). After induction by doxycycline, type 2 diabetes mellitus (370.0 ± 21.4 mg/dl) and hypertensive, type 2 diabetes mellitus rats (367.6 ± 20.1 mg/dl) exhibited higher blood glucose levels, whereas blood glucose levels in the hypertensive (110.3 ± 4.7 mg/dl) and SD controls (108.5 ± 3.3 mg/dl) were within normal limits (Fig. 1D).

The tetO-shIR rats also had hyperinsulinemia and increased C-peptide levels (data not shown). Echocardiographic assessment of the different models revealed a higher wall thickness (Fig. 2A) calculated by thickness of septum (IVSd) and posterior wall of the LV (LVPWd) in hypertensive mRen27 rats (4.6 ± 0.2 mm) while SD (3.5 ± 0.1 mm), diabetic (2.3 ± 0.1 mm), and hypertensive diabetic rats (3.0 ± 0.2 mm) had no thickened cardiac walls (Fig. 2A). The ejection fraction (Fig. 2B) and fractional shortening (Fig. 2C) values were slightly, but significantly reduced in both diabetic (EF $42.8 \pm 4.0\%$, FS $21.8 \pm 1.4\%$) and hypersensitive rats (EF $39.2 \pm 2.7\%$, FS $15.4 \pm 1.8\%$) compared to SD rats (EF $60.1 \pm 2.1\%$, FS $31.9 \pm 1.4\%$). Systolic heart function was further diminished in the hypertensive type 2 diabetes mellitus rats (EF $28.2 \pm 3.0\%$, FS $15.0 \pm 2.1\%$).

Two-dimensional speckle tracking echocardiography-derived measurement of LV strain and strain rate was performed to examine LV myocardial performance. Global longitudinal strain (GLS, Fig. 2D), global radial strain (GRS, Fig. 2E), and global circumferential strain (GCS, Fig. 2F) were significantly decreased in diabetic (GLS $-10.4 \pm 1.0\%$, GRS $15.2 \pm 1.4\%$, GCS $-16.3 \pm 1.2\%$), hypersensitive (GLS $-11.2 \pm 0.8\%$, GRS $19.3 \pm 2.1\%$, GCS $-9.7 \pm 1.1\%$) and hypertensive diabetic rats (GLS $-5.5 \pm 0.6\%$, GRS $8.8 \pm 1.1\%$, GCS $-7.6 \pm 0.8\%$) compared with SD rats (GLS $-19.1 \pm 0.7\%$, GRS $28.5 \pm 3.2\%$, GCS $-19.3 \pm 0.5\%$). Similar results were observed for the respective global strain rates (data not shown).

According our empa study design (Fig. 3A), we investigated the effects of empa on the cardiac target-organ damage in the hypertensive diabetic rats (mRen27/tetO-shIR). The survival rates (Fig. 3B) during the 4 weeks of treatment were unchanged between the empa (70.0%) and vehicle group (68.4%). Treatment of the hypertensive diabetic rats by empa had no effect on the blood pressure (Fig. 3C). Empa treatment led to significant lower blood glucose level (Fig. 3D). Glucose level decreased from 359.4 ± 35.8 mg/dl in vehicle treated rats to 182.3 ± 10.4 mg/dl in empa treated ones. The drinking volumes of empa treated rats were unaltered compared to the vehicle group (Fig. 3E).

We then assessed the effect of empa on cardiac function by echocardiography. No effects of empa treatment on wall thickness could be detected (Fig. 4A). Empa significantly increased the ejection fraction ($42.8 \pm 4.0\%$) and fractional shortening ($22.6 \pm 2.9\%$) compared to vehicle treated hypertensive diabetic rats (Fig. 4B-C). Moreover, empa has a positive effect on all 3 global strains. Global longitudinal ($-8.5 \pm 0.5\%$), radial ($20.4 \pm 2.7\%$) and circumferential ($-11.0 \pm 0.7\%$) strains were significantly enhanced by empa treatment compared to the vehicle group (Fig. 4D-F). Similar results were observed for the global longitudinal and radial strain rates (data not shown).

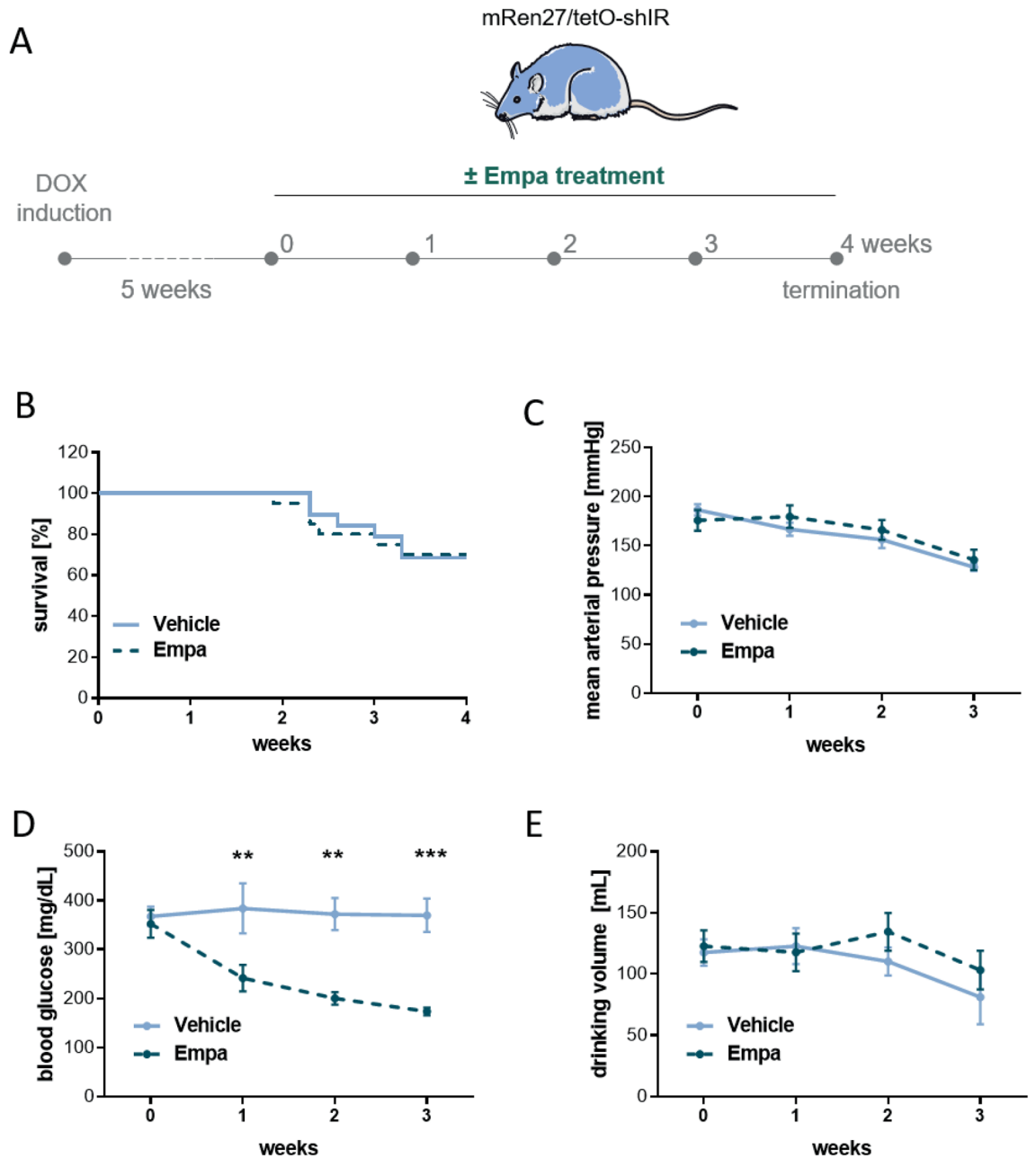


Figure 3. Study design and outcome after empa treatment. (A) Experimental flow chart of EMPA study design. (B) Kaplan–Meier survival analysis showed no effect of empa treatment on survival and no effect on (C) mean arterial blood pressure. (D) Blood glucose level were significantly reduced by empa during the treatment period. (E) Empa treatment had no effect on the drinking volume. 2-way ANOVA, ** $p < 0.01$, *** $p < 0.001$; data expressed as mean \pm SEM.

The mRNA expression level of the cardiac marker *Anp* (1.37 ± 0.45 vs. 1.17 ± 0.20), *Bnp* (1.10 ± 0.05 vs. 1.26 ± 0.12), *Fn* (1.57 ± 0.31 vs. 0.93 ± 0.19) and *Ctgf* (0.99 ± 0.12 vs. 0.82 ± 0.08) were unchanged. Only an increase in the ratio of *Myh6/Mhy7* mRNA expression in empa treated rats (0.14 ± 0.05) compared to vehicle treated animals (0.40 ± 0.09) were detectable (Fig. 4G). Additionally, we analyzed circulating BNP levels that were also unaltered by empa treatment (data not shown). Immunohistochemical staining for cardiac macrophage infiltration (ED1), interstitial (fibronectin) and perivascular fibrosis (collagen I) was also investigated. Macrophage infiltration (Fig. 5A) was decreased in the cardiac tissue in the empa treated rats (22.4 ± 1.7 per fov) compared to vehicle treated (32.3 ± 2.3 per fov) whereas interstitial (Fig. 5B) and perivascular (Fig. 5C) fibrosis was not affected by empa treatment.

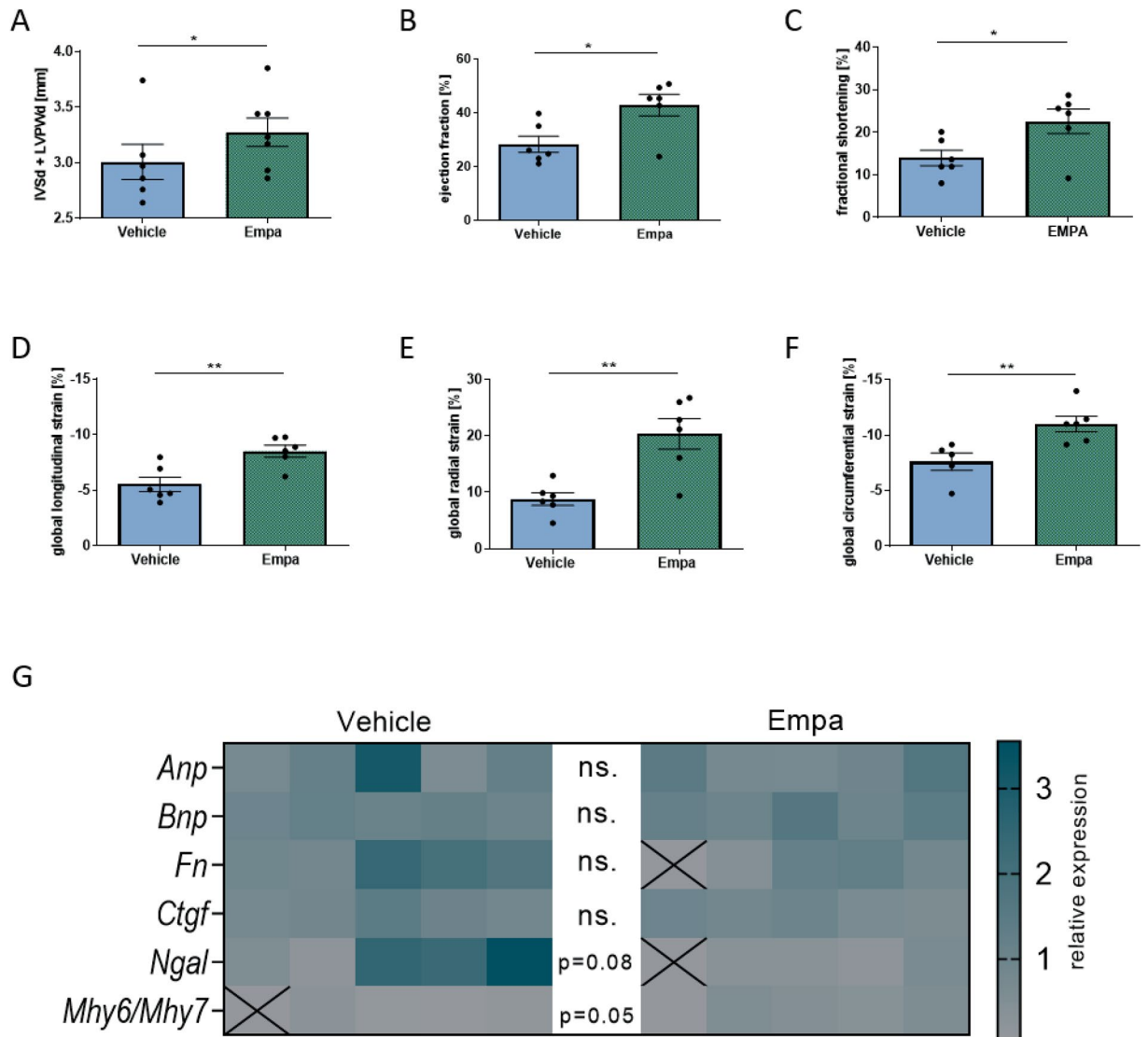


Figure 4. Speckle Trackle Echocardiography and gene expression analysis after empagliflozin treatment. (A) No effects of empagliflozin treatment on wall thickness could be detected. (B) Ejection fraction and (C) fractional shortening were significantly increased by empagliflozin. (D) Global longitudinal strain was significantly elevated by empagliflozin treatment, as were (E) global radial strain and (F) global circumferential. (G) Heatmap of gene expression values in relation to 18S housekeeper are shown for every single animal. Relative gene expression is illustrated in corresponding color. Statistical outliers are marked with X. There is no change in cardiac atrial natriuretic peptide (*Anp*), brain natriuretic peptide (*Bnp*), fibronectin (*Fn*) or connective tissue growth factor (*Ctgf*) mRNA expression due to empagliflozin treatment. The ratio of alpha (*Mhy6*) and beta myosin heavy chain (*Mhy7*) mRNA expression is increased by treatment. Students t-test, * $p < 0.05$ ** $p < 0.01$; data expressed as mean \pm SEM.

Discussion

We investigated the combined effects of hypertension and hyperglycemia on end-organ damage, focusing on the heart. We used a well-established transgenic rat model, overexpressing the mouse salivary-gland renin gene. This model is based on increased angiotensin II production resulting in a rightward shift in the pressure natriuresis curve¹⁸. We crossed these animals with a unique tetracycline-inducible type 2 diabetes mellitus technique where insulin resistance results from downregulation of the insulin receptor¹¹. Almost two third of the hypertensive type 2 diabetes mellitus rats died between week 6 and 9 in our experiment, underscoring the lethality of hypertension plus hyperglycemia-induced heart failure. Surviving rats that could be measured had a marked reduction of systolic function and the worst global longitudinal strain, radial strain, and circumferential strain, thus we have introduced a novel model of two step heart failure (HF). In most rodent HF models, HF develops gradually over time due to a single stimulus. However, in human HF multiple factors are involved and trigger decompensation episodes. Among these factors, arterial hypertension is a prevalent trigger for decompensation episodes. We succeeded in establishing a novel HF rat model, which combines two incumbent protocols to achieve both the development of HF and the possibility to add a second stimulus to induce (HFREF).

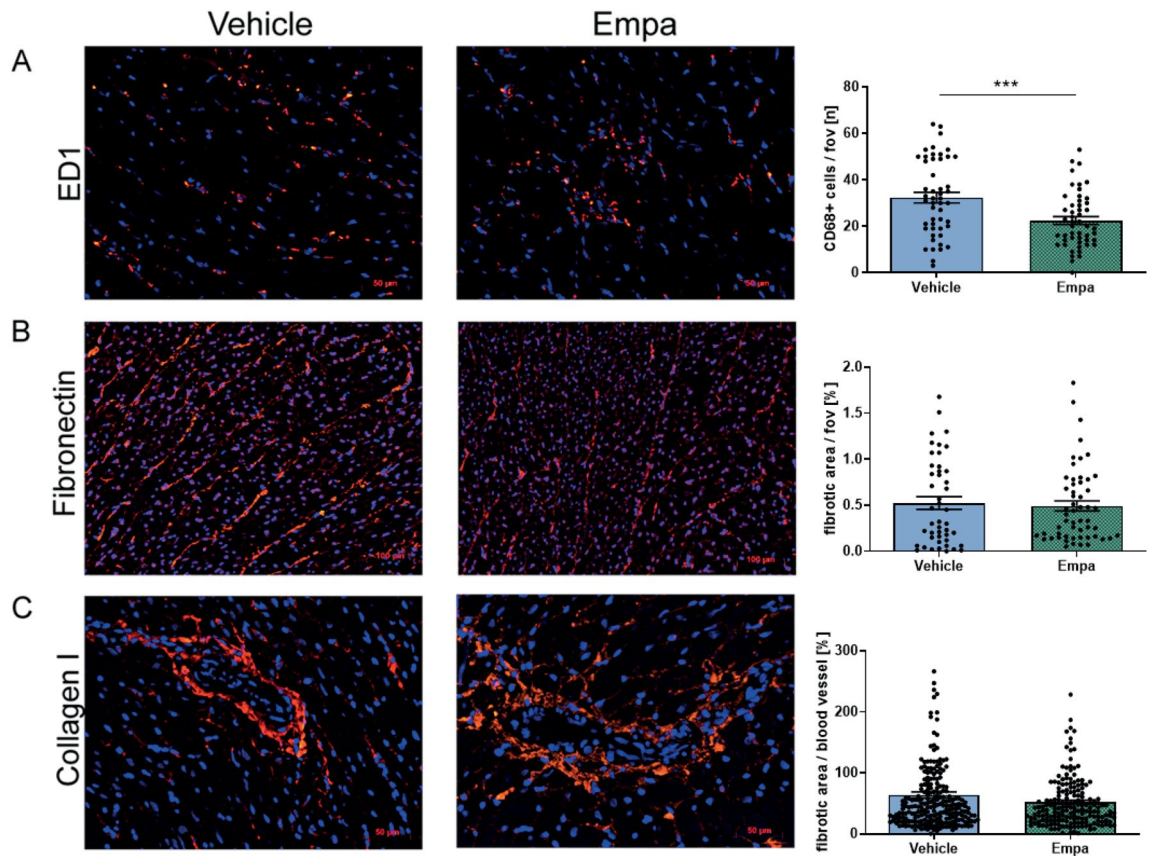


Figure 5. Protein expression after empagliflozin treatment. (A) Representative image of ED-1 IHC staining for macrophages in the heart from empagliflozin and vehicle-treated rats. The number of macrophages was decreased in the heart of empagliflozin treated rats. (B) Representative image of fibronectin IHC staining in the hearts from empagliflozin and vehicle-treated rats. Interstitial cardiac fibrosis was estimated as fibronectin-positive area per view field. Heart sections of empagliflozin and vehicle-treated rats showed no differences in cardiac interstitial fibrosis. (C) Representative image of collagen I IHC staining in the hearts from empagliflozin and vehicle-treated rats. Perivascular fibrosis area was normalized to vessel media cross-sectional area. Heart sections of empagliflozin and vehicle-treated rats showed no differences in cardiac perivascular fibrosis. Students t-test, *** $p < 0.001$; data expressed as mean \pm SEM.

Hypertensive diabetic rats as a model have been investigated earlier. Iams and Wexler produced diabetes with alloxan in spontaneously hypertensive rats (SHR) in 1977¹⁹. Mortality was high and animals became cachectic and moribund, probably related to acute metabolic disturbances rather than target-organ damage. The authors did not report data regarding blood pressure. Streptozotocin has also been commonly given to SHR. Hori et al.²⁰ reported on basement membrane changes in various tissue but also did not report on blood pressure-related effects. Techniques designed to destroy islet beta cells are more akin to type 1 diabetes mellitus rather than type 2 diabetes mellitus. Rats with type 2 diabetes mellitus present a significant challenge. Most rodent models are genetically or chemically modified to produce diabetes. Commonly high-fat-feeding is required, the length of time to develop diabetes is quite long and the phenotype is variable. The Nile rat may be an exception²¹. Nile rats develop diabetes within 8–10 weeks with high-carbohydrate diet similar to humans, and are protected by high-fat, low-glycemic load intake²¹. That model, with less carefully defined insulin levels, proved unpractical for our purposes. Thus, we selected the tetO-shIR rat, which allowed us to avoid additional dietary manipulations. Another unique advantage is that the type 2 diabetes mellitus can be turned on and off with tetracycline.

We tested the hypothesis if empagliflozin will be protective in a heart failure model which is not based on a primary vascular event. Controls were mRen27/tetO-shIR given vehicle. Empa lowered plasma glucose levels from 400 mg/dL to under 200 mg/dL, a remarkable reduction based on increased glucose excretion alone. Blood pressure was not changed by this treatment. Nonetheless, empagliflozin improved cardiac function by increasing ejection fraction and fractional shortening compared to vehicle-treated controls. Moreover, empagliflozin has a positive effect on all 3 global strains. Global longitudinal, radial, and circumferential strains were significantly enhanced by empagliflozin treatment compared to the vehicle group. Since no cardiac expression of SGLT2 receptors has been described, it is difficult to postulate any direct effect of the drug on the myocardium per se. However, it is possible that empagliflozin binds to myocardial receptors or substrates other than SGLT2. In our model the improvement in systolic and diastolic function was not secondary to a reduction in left ventricular mass or through modification of the afterload since blood pressure was not changed.

Empa has been previously studied in other rodent models of hypertension and diabetes. Younis et al. studied the Cohen Rosenthal diabetic hypertensive rat²². This model is an SHR cross with the Cohen diabetic rat. Unlike

in our model empag lowered blood pressure by 15 mmHg and also reduced left ventricular mass and systolic dilation. Steven et al. also reported favorable results in the Zucker diabetic fatty rat²³. They found that endothelial function was improved and inflammatory markers were reduced. Similarly, Zhou and Wu observed that empag treatment in streptozotocin-induced diabetes reduced serum glucose, while improving cardiac function and lowering expression of glucose-regulated protein-78 and enhancer-binding protein homologous protein²⁴. Thus, it is obvious that several, putative mechanisms underlying SGLT2 inhibitor-associated cardiovascular benefits occur as in patients as in rodents.

Whether or not the mechanism(s) involved in glycemic control and cardiovascular risk reduction are dissociated and/or follow a different dose–response-curve is unclear. Due to the profound and early effects of empag on HF in patients and the fact that they were not due to improvement in atherothrombotic complications (myocardial infarction and stroke remained unchanged), it is difficult to ascribe all these salubrious effects solely to serum glucose reduction²⁵.

Ascribing the favorable effects to altered ventricular loading conditions secondary to a reduction in preload primarily due to the diuretic and natriuretic effects is an alternative mechanism. SGLT2 inhibition in the proximal tubule leads to natriuresis and glucosuria, and the ensuing osmotic diuresis may be favorable, particularly in the diabetic and hypertensive heart, which functions on a steep Frank-Starling curve. We observed no effects of empag on drinking volume, although we could not monitor daily urinary output. This must be kept in mind when comparing the circulating volumes. In patients with heart failure, a differential effect in the regulation of interstitial fluid (versus intravascular volume) may be particularly important, in many of whom there is intravascular contraction, often exacerbated by diuresis. The ability to selectively reduce interstitial fluid may be a unique feature of SGLT2 inhibitors. Other diuretic SGLT2 inhibitors may directly inhibit the Na⁺/H⁺ exchanger 1 isoform in the myocardium^{26,27}, reduced cytoplasmic sodium and calcium levels, while increasing mitochondrial calcium levels.

SGLT2 inhibitors have shown to optimize cardiac energy metabolism and subsequently improve myocardial energetics and substrate efficiency. In a recent study empagliflozin increased ketone consumption, reduced cardiac lactate production and glucose consumption after myocardial infarction in pigs²⁸. Alternatively empag inhibits the Na⁺/H⁺ exchanger, lowering cytosolic sodium and calcium levels and increasing mitochondrial calcium concentrations²⁷.

Taken together, our observations suggest the potential of empagliflozin to favorably promote left ventricular reverse remodeling and improve diastolic function in patients with type 2 diabetes and hypertension induced cardiovascular disease. A trial to test the effects of empag on the heart in patients is underway²⁹. There is a reason to be optimistic since only SGLT2 inhibitors and glucagon-like peptide 1 agonists have been shown to have favorable effects on reducing mortality in type 2 diabetes mellitus patients³⁰.

Conclusion

The EMPA-REG OUTCOME trial documented impressive empagliflozin benefits on heart failure in diabetic patients with cardiovascular disease. A cardiovascular protective effect was more primary on preventing systolic heart failure morbidity and mortality than on preventing vascular events such as stroke and acute myocardial infarction. New ESC guidelines on chronic coronary syndromes favor SGLT2 inhibitors as primary medication in untreated patients with diabetes before introducing metformin. The key question of this study was if empagliflozin will be protective in a heart failure model which is not induced by a primary vascular event, such as myocardial infarction, leading to heart failure with reduced ejection fraction. Therefore, we developed an innovative rodent model for HFpEF which progresses to heart failure with mildly reduced ejection fraction. Empagliflozin ameliorated cardiovascular dysfunction in this model. The beneficial effect was not secondary to a reduction in LV mass or through modulation of the blood pressure. In future, SGLT2 inhibitors will become an important primary vascular preventive pillar next to lipid lowering and platelet inhibition independent of the diagnosis diabetes. Future studies will determine the exact mode of action and the patient groups with chronic coronary syndrome and heart failure who will benefit most.

Data availability

The datasets used and analysed during the current study are available from the corresponding author on reasonable request.

Received: 14 February 2020; Accepted: 23 June 2020

Published online: 20 August 2020

References

- Writing group, M. et al. Executive summary: heart disease and stroke statistics-2016 update: a report from the American Heart Association. *Circulation* **133**, 447–454. <https://doi.org/10.1161/CIR.0000000000000366> (2016).
- Fox, C. S. Cardiovascular disease risk factors, type 2 diabetes mellitus, and the Framingham Heart Study. *Trends Cardiovasc. Med.* **20**, 90–95. <https://doi.org/10.1016/j.tcm.2010.08.001> (2010).
- McMurray, J. J. & Pfeffer, M. A. Heart failure. *Lancet* **365**, 1877–1889. [https://doi.org/10.1016/S0140-6736\(05\)66621-4](https://doi.org/10.1016/S0140-6736(05)66621-4) (2005).
- Komajda, M. et al. Heart failure events with rosiglitazone in type 2 diabetes: data from the RECORD clinical trial. *Eur. Heart J.* **31**, 824–831. <https://doi.org/10.1093/eurheartj/ehp604> (2010).
- Scirica, B. M. et al. Heart failure, saxagliptin, and diabetes mellitus: observations from the SAVOR-TIMI 53 randomized trial. *Circulation* **132**, e198. <https://doi.org/10.1161/CIR.0000000000000330> (2015).
- Nathan, D. M. Diabetes: advances in diagnosis and treatment. *JAMA* **314**, 1052–1062. <https://doi.org/10.1001/jama.2015.9536> (2015).
- Zinman, B. et al. Empagliflozin, cardiovascular outcomes, and mortality in type 2 diabetes. *N. Engl. J. Med.* **373**, 2117–2128. <https://doi.org/10.1056/NEJMoa1504720> (2015).

8. Sattar, N., McLaren, J., Kristensen, S. L., Preiss, D. & McMurray, J. J. SGLT2 Inhibition and cardiovascular events: why did EMPA-REG Outcomes surprise and what were the likely mechanisms?. *Diabetologia* **59**, 1333–1339. <https://doi.org/10.1007/s00125-016-3956-x> (2016).
9. Verma, S. & McMurray, J. J. V. SGLT2 inhibitors and mechanisms of cardiovascular benefit: a state-of-the-art review. *Diabetologia* **61**, 2108–2117. <https://doi.org/10.1007/s00125-018-4670-7> (2018).
10. Knuuti, J. *et al.* ESC Guidelines for the diagnosis and management of chronic coronary syndromes. *Eur. Heart J.* <https://doi.org/10.1093/eurheartj/ehz425> (2019).
11. Kotnik, K. *et al.* Inducible transgenic rat model for diabetes mellitus based on shRNA-mediated gene knockdown. *PLoS ONE* **4**, e5124. <https://doi.org/10.1371/journal.pone.0005124> (2009).
12. Langheinrich, M. *et al.* The hypertensive Ren-2 transgenic rat TGR (mREN2)27 in hypertension research. Characteristics and functional aspects. *Am. J. Hypertens* **9**, 506–512 (1996).
13. Houser, S. R. *et al.* Animal models of heart failure: a scientific statement from the American Heart Association. *Circ. Res.* **111**, 131–150. <https://doi.org/10.1161/RES.0b013e3182582523> (2012).
14. Susic, D. & Frohlich, E. D. Hypertensive cardiovascular and renal disease and target organ damage: lessons from animal models. *Cardiorenal Med.* **1**, 139–146. <https://doi.org/10.1159/000329334> (2011).
15. Kraker, K. *et al.* Statins reverse postpartum cardiovascular dysfunction in a rat model of preeclampsia. *Hypertension* **75**, 202–210. <https://doi.org/10.1161/HYPERTENSIONAHA.119.13219> (2020).
16. Wilck, N. *et al.* Nitric oxide-sensitive guanylyl cyclase stimulation improves experimental heart failure with preserved ejection fraction. *JCI Insight* <https://doi.org/10.1172/jci.insight.96006> (2018).
17. Haase, N. *et al.* Relaxin does not improve Angiotensin II-induced target-organ damage. *PLoS ONE* **9**, e93743. <https://doi.org/10.1371/journal.pone.0093743> (2014).
18. Gross, V., Lippoldt, A., Schneider, W. & Luft, F. C. Effect of captopril and angiotensin II receptor blockade on pressure natriuresis in transgenic TGR(mRen-2)27 rats. *Hypertension* **26**, 471–479 (1995).
19. Iams, S. G. & Wexler, B. C. Alloxan diabetes in spontaneously hypertensive rats: gravimetric, metabolic and histopathological alterations. *Br. J. Exp. Pathol.* **58**, 177–199 (1977).
20. Hori, S., Nishida, T., Mukai, Y., Pomeroy, M. & Mukai, N. Ultrastructural studies on choroidal vessels in streptozotocin-diabetic and spontaneously hypertensive rats. *Res. Commun. Chem. Pathol. Pharmacol.* **29**, 211–228 (1980).
21. Subramaniam, A., Landstrom, M., Luu, A. & Hayes, K. C. The Nile rat (*Arvicanthis niloticus*) as a superior carbohydrate-sensitive model for type 2 diabetes mellitus (T2DM). *Nutrients* <https://doi.org/10.3390/nu10020235> (2018).
22. Younis, F. *et al.* Beneficial effect of the SGLT2 inhibitor empagliflozin on glucose homeostasis and cardiovascular parameters in the Cohen Rosenthal Diabetic Hypertensive (CRDH) rat. *J. Cardiovasc. Pharmacol. Ther.* **23**, 358–371. <https://doi.org/10.1177/1074248418763808> (2018).
23. Steven, S. *et al.* The SGLT2 inhibitor empagliflozin improves the primary diabetic complications in ZDF rats. *Redox Biol.* **13**, 370–385. <https://doi.org/10.1016/j.redox.2017.06.009> (2017).
24. Zhou, Y. & Wu, W. The sodium-glucose co-transporter 2 inhibitor, empagliflozin, protects against diabetic cardiomyopathy by inhibition of the endoplasmic reticulum stress pathway. *Cell Physiol. Biochem.* **41**, 2503–2512. <https://doi.org/10.1159/000475942> (2017).
25. McMurray, J. EMPA-REG—the “diuretic hypothesis”. *J Diabetes Comp.* **30**, 3–4. <https://doi.org/10.1016/j.jdiacomp.2015.10.012> (2016).
26. Packer, M., Anker, S. D., Butler, J., Filippatos, G. & Zannad, F. Effects of sodium-glucose Cotransporter 2 inhibitors for the treatment of patients with heart failure: proposal of a novel mechanism of action. *JAMA Cardiol.* **2**, 1025–1029. <https://doi.org/10.1001/jamacardio.2017.2275> (2017).
27. Uthman, L. *et al.* Class effects of SGLT2 inhibitors in mouse cardiomyocytes and hearts: inhibition of Na(+)/H(+) exchanger, lowering of cytosolic Na(+) and vasodilation. *Diabetologia* **61**, 722–726. <https://doi.org/10.1007/s00125-017-4509-7> (2018).
28. Santos-Gallego, C. G. *et al.* Empagliflozin induces a myocardial metabolic shift from glucose consumption to ketone metabolism that mitigates adverse cardiac remodeling and improves myocardial contractility. *J. Am. Coll. Cardiol.* [https://doi.org/10.1016/s0735-1097\(18\)31215-4](https://doi.org/10.1016/s0735-1097(18)31215-4) (2018).
29. Natali, A., Nesti, L., Fabiani, I., Calogero, E. & Di Bello, V. Impact of empagliflozin on subclinical left ventricular dysfunctions and on the mechanisms involved in myocardial disease progression in type 2 diabetes: rationale and design of the EMPA-HEART trial. *Cardiovasc. Diabetol* **16**, 130. <https://doi.org/10.1186/s12933-017-0615-6> (2017).
30. Zheng, S. L. *et al.* Association between use of sodium-glucose cotransporter 2 inhibitors, glucagon-like peptide 1 agonists, and dipeptidyl peptidase 4 inhibitors with all-cause mortality in patients with type 2 diabetes: a systematic review and meta-analysis. *JAMA* **319**, 1580–1591. <https://doi.org/10.1001/jama.2018.3024> (2018).

Acknowledgements

We thank Ute Gerhard, Juliane Anders, May-Britt Köhler, Jutta Meisel, Astrid Schiche, Reika Langanki and Ralph Plehm and for their excellent technical assistance. Images were modified from Smart Servier Medical Art, Les Laboratoires Servier (<https://creativecommons.org/licenses/by/3.0/legalcode>). The Deutsche Forschungsgemeinschaft (DFG) supported FH (HE 6249/4-1, HE 6249/5-1), and RD (DE 631/9-1), as well as DNM, NA and MB by SFB1365. Grants in aid from Boehringer Ingelheim.

Author contributions

Conception and design of the research: K.K., F.H., R.D.; acquisition of data: K.K., MG and ME; Validation: SCG and JG; Formal Analysis: KK, FH and NH.; Investigation: MG, ME and AH; Data Curation: KK and FH; Writing – Original Draft Preparation: KK and FH; Writing – Review: MG, NR, SCG, OS, JG, UK, ME, MB, NA, AH, FCL, DNM, RD and NH. Visualization: KK, FH and NH; Supervision: OS, UK, MB, FCL, DNM and RD; Project Administration: KK, FH, MG and ME; Funding Acquisition: RD. All authors read and approved the final manuscript.

Funding

Open access funding provided by Projekt DEAL.

Competing interests

RD has served as advisor for Boehringer Ingelheim and has lectured on empagliflozin. UK took part on an Advisory Board from Boehringer Ingelheim. The rest of the authors have no competing interests.

Additional information

Supplementary information is available for this paper at <https://doi.org/10.1038/s41598-020-70708-5>.

Correspondence and requests for materials should be addressed to R.D.

Reprints and permissions information is available at www.nature.com/reprints.

Publisher's note Springer Nature remains neutral with regard to jurisdictional claims in published maps and institutional affiliations.



Open Access This article is licensed under a Creative Commons Attribution 4.0 International License, which permits use, sharing, adaptation, distribution and reproduction in any medium or format, as long as you give appropriate credit to the original author(s) and the source, provide a link to the Creative Commons license, and indicate if changes were made. The images or other third party material in this article are included in the article's Creative Commons license, unless indicated otherwise in a credit line to the material. If material is not included in the article's Creative Commons license and your intended use is not permitted by statutory regulation or exceeds the permitted use, you will need to obtain permission directly from the copyright holder. To view a copy of this license, visit <http://creativecommons.org/licenses/by/4.0/>.

© The Author(s) 2020